

Thermal Management of Micro-Hotplates using MEMCAD as Simulation Tool

D. Briand, M.-A. Grétilat, B. van der Schoot and N.F. de Rooij

Institute of Microtechnology, Rue Jaquet-Droz 1, P.O. Box 3,
CH-2007 Neuchâtel, Switzerland, danick.briand@imt.unine.ch

ABSTRACT

In this paper we report on the electrothermal simulations performed in the aim of optimising the power consumption and the temperature distribution of micro-hotplates for gas sensing applications. The micro-hotplate designs were optimised using the software MEMCAD from Microcosm Technologies. From the results obtained, we propose a micro-hotplate design with a silicon island underneath the membrane. The silicon island ensures a uniform temperature over the sensing area for the metal-oxide gas sensors. Moreover, it allows to thermally isolating electronic components and was used to lower the power consumption of MOSFET gas sensors. The optimised micro-hotplates are suitable for applications in the automotive industry and in electronic nose instruments.

Keywords: Micro-Hotplates, FEM Simulation, MEMCAD, Thermal, Gas sensors.

1 INTRODUCTION

Micro-hotplates are of great interest in the field of gas sensors since they allow the reduction of the power consumption and new modes of operation [1-3]. The main characteristics to optimise for such devices are the power consumption, the temperature distribution over the sensing area and the robustness. FEM simulation is a useful tool to simulate the thermal properties of such devices. So far, the main CAD packages used for this purpose are ANSYS, SESES, COSMOS and SOLIDIS [4-8].

During the last years we have reported on the fabrication and the characterisation of micro-hotplates for metal-oxide and for MOSFET gas sensors [9-11]. Both micro-hotplate types have been designed and optimised using the MEMCAD (4.5) FEM simulation tool from Microcosm Technologies, Inc [12]. The Mechanical-Electro-Thermal module (MemEThem) was used to simulate the thermal behaviour of the devices. This Joule heating module computes the thermal and electrical potential field distributions resulting from an applied voltage or current through a resistive element. The mechanical coupling was not included in the simulations, but can be of interest in the case of designing thermal actuators [13]. The simulation manager (SimMan) was used to investigate the influence of the dimensions on the micro-hotplates thermal properties. Thermal measurements were

performed and combined with the simulations, the values of the convection and thermal conductivity coefficients were defined.

The micro-hotplates for the metal-oxide gas sensors were first designed in the aim of withstanding the high temperature required for the drop coating procedure of the gas sensitive material [9]. Since then FEM simulations have been performed to optimise the temperature distribution over the sensing area, which has a strong influence on the sensitivity and selectivity of the sensor. In this communication, we present a micro-hotplate design having a silicon island underneath the membrane. The silicon island provides a homogeneous temperature over the sensing area and allows to thermally isolate electronic components.

2 DESIGN AND FABRICATION

2.1 Micro-hotplates for metal-oxide sensors

The micro-hotplates for the metal-oxide gas sensors consist of a heater stacked between a membrane and an insulator covered with electrodes. A low-stress LPCVD silicon nitride film is used as membrane and insulator. The heater (100 Ω) and the electrodes are made of platinum (TCR=0.0020/ $^{\circ}$ C). Backside silicon micromachining is used to release the dielectric membrane, which thermally isolates the heated sensing area from the chip frame (Fig 1). More details concerning the design and the fabrication can be found in ref. [14].

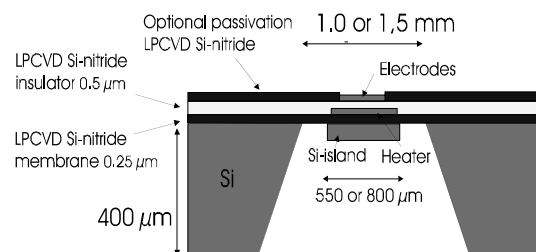


Figure 1: Micro-hotplate for metal-oxide gas sensors with an optional silicon island.

2.2. Micro-hotplates for MOSFET sensors

The micro-hotplates with thermally isolated electronic components have also a membrane made of low-stress

LPCVD nitride, which is released using a two steps silicon bulk micromachining process [10-11]. The heater is a semiconducting resistor implanted in the silicon island. A diode is used as temperature sensor. The metallisation is made of aluminium and covered with a PECVD silicon oxynitride film.

An array of 4 MOSFET gas sensor [15] are located in the silicon island and therefore thermally isolated from the chip frame (Fig. 2). Windows are opened on the MOSFET gate oxide and catalytic metal films such as Ir, Pt, Pd replace the gate.

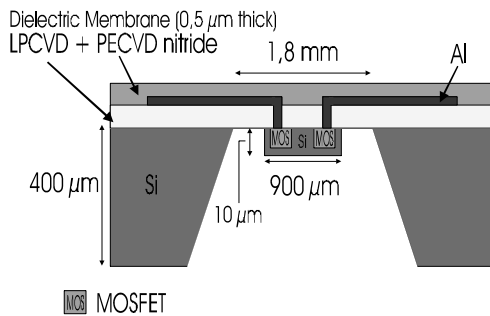


Figure 2: Micro-hotplates for MOSFET gas sensors.

3 EXPERIMENT

3.1 Characterisation

The device temperature was measured using an infrared camera AVIO 2100, with a pixel resolution of $12.5 \times 20 \mu\text{m}^2$. The IR thermal measurements were performed on the micro-hotplates in ambient atmosphere and in vacuum. The resistance dependence on the voltage and the maximum temperature under these conditions were monitored. The power consumption was directly obtained from these measurements. The later in combination with the simulator were used to define the convection coefficients.

3.2 Optimisation and simulations

Concerning the micro-hotplates for metal-oxide gas sensors, the power consumption was lowered adjusting the membrane and the heater size. Two membrane sizes were investigated: $1.0 \times 1.0 \text{ mm}^2$ and $1.5 \times 1.5 \text{ mm}^2$ with respectively a heater and sensing area of $500 \times 500 \mu\text{m}^2$ and $750 \times 750 \mu\text{m}^2$. The temperature distribution over the sensing area was optimised by studying different heater geometry such as simple and double meander. Moreover, a $\cong 10 \mu\text{m}$ thick silicon (thermal conductivity 100 times higher than oxide) island was added underneath the membrane to improve the temperature homogeneity over the sensing area (Fig. 1). A thickness of $10 \mu\text{m}$ was chosen due to the fabrication process, which offers a limited control on the silicon island thickness [10, 14]. However,

simulations were performed to determine the minimum thickness of silicon necessary to have a uniform temperature distribution over the sensing area.

Simulations have been performed using the following boundary conditions:

- The chip frame temperature was set at 30°C according to the IR observations;
- The heat is dissipated through convection in the gaseous atmosphere on the front and backside surface of the membrane;
- The radiation was considered negligible [6];
- A heater voltage of 2.5 V (if not mentioned) corresponding to an operating temperature of about $250\text{-}350^\circ\text{C}$;
- A membrane size = $1.5 \times 1.5 \text{ mm}^2$, heating and sensing area = $750 \times 750 \mu\text{m}^2$, silicon island area = $800 \times 800 \mu\text{m}^2$;
- Thickness of the Si_3N_4 membrane = $0.25 \mu\text{m}$, thickness of the Pt heater = $0.25 \mu\text{m}$.

The convection coefficients were set respectively for the front and the backside of the membrane at 125 and $60 \text{ W}\cdot\text{m}^{-2}\text{K}^{-1}$. The thermal conductivity coefficients of the films were taken from literature [6, 16]. The thermal conductivity of the silicon rich LPCVD nitride film was set at $3 \text{ W}\cdot\text{m}^{-1}\text{K}^{-1}$, the platinum at $70 \text{ W}\cdot\text{m}^{-1}\text{K}^{-1}$ and the silicon at $150 \text{ W}\cdot\text{m}^{-2}\text{K}^{-1}$.

4 RESULTS AND DISCUSSION

4.1 Thermal measurements

Figure 3 presents the variation of the temperature as a function of the power consumption for micro-hotplates with a membrane area respectively of 1.0×1.0 and $1.5 \times 1.5 \text{ mm}^2$. At an operating temperature of 300°C , their power consumption is respectively 55 and 75 mW . The convection losses correspond to $\approx 70\%$ of the total heat dissipated.

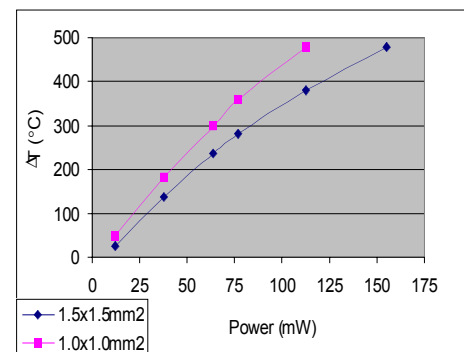


Figure 3: Temperature variation as a function of the power consumption in air for $1.0 \times 1.0 \text{ mm}^2$ micro-hotplate with a heating area of $500 \times 500 \mu\text{m}^2$ and $1.5 \times 1.5 \text{ mm}^2$ micro-hotplate with a heating area of $750 \times 750 \mu\text{m}^2$.

The micro-hotplates with a membrane area of $1.0 \times 1.0 \text{ mm}^2$ consume less than the ones with a membrane of $1.5 \times 1.5 \text{ mm}^2$. This could be explained by their smaller heating area, which reduces the absolute heat lost by convection. A way to optimise the power consumption is to minimise the heating area in relation with the membrane size, therefore to combine a heating area of $500 \times 500 \text{ }\mu\text{m}^2$ with a membrane size of $1.5 \times 1.5 \text{ mm}^2$. This way it is also possible to reduce the power lost by convection and by conduction through the membrane as shown before by different research groups [4, 5, 6].

The power consumption for micro-hotplates having a $10 \text{ }\mu\text{m}$ thick silicon island was about 20 % higher at an operating temperature of 300°C . The heat dissipated could be reduced by optimising the thickness of the silicon island.

4.2 Optimisation using FEM simulations

About the micro-hotplates without silicon islands, the thermal observations have shown that the temperature distribution over the sensing area was more homogeneous for the double meander heater compared to the simple meander. The FEM simulations have confirmed this experimental result. Depending on the applications, different heater geometry has been proposed during the years [6, 17, 18].

Although, the temperature gradient between the centre and the edge of the sensing area can reach a value up to 80°C for a simple meander heater (Fig. 7). A $10 \text{ }\mu\text{m}$ thick silicon (thermal conductivity 100 times higher than oxide) island was then added underneath the membrane to improve the temperature homogeneity over the sensing area, as shown by FEM simulations (Fig. 4 compared to Fig. 5).

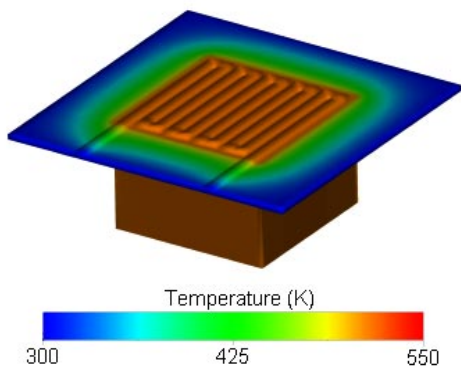


Figure 4: FEM simulation of the micro-hotplates with a silicon island added (z-axis x 50, Si-island thickness= $10 \text{ }\mu\text{m}$)

Using this design ($10 \text{ }\mu\text{m}$ thick silicon island), the temperature distribution over the sensing area is uniform ($\pm 1^\circ\text{C}$ all over the silicon island surface) for any heater geometry. Moreover, the heater and the electrodes (Pt) can be defined in one fabrication step using the same mask level.

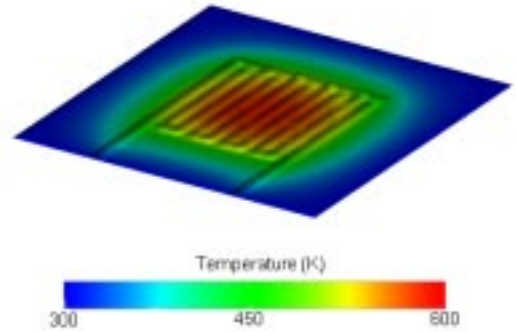


Figure 5: Micro-hotplates thermal FEM simulations with a simple meander heater and no silicon island underneath the membrane.

This micro-hotplate design was also used to lower the power consumption of MOSFET gas sensors [10, 11]. A semiconducting heater having a U shape was adopted giving more flexibility in the layout, an important issue due to the high number of electrical connections. Figure 6 shows the homogeneous temperature distribution on the sensing area for a heater with a U shape on a silicon nitride membrane with a silicon island. The heater was made of platinum to simplify the simulation.

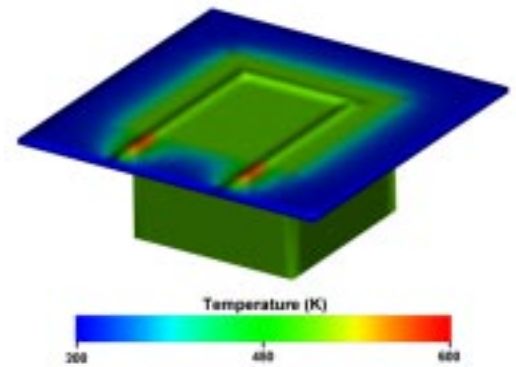


Figure 6: Micro-hotplates thermal FEM simulations with a U shape heater and a silicon island (z-axis x 50, Si-island thickness= $10 \text{ }\mu\text{m}$, voltage = 2 V).

An optimisation of the silicon island thickness to minimise the power consumption and still obtain a uniform temperature over the sensing area was performed. The metal-oxide gas sensor with a simple meander heater and the MOSFET sensor having a heater with a U shape were considered. The shape of the heater and the operating temperature influences the temperature gradient on the sensing area. The simulations were performed in respect with the operating temperature of the metal-oxide (300°C) and MOSFET gas sensors (225°C). In the case of the metal-oxide sensor, the temperature gradient has to be minimised ($< 25^\circ\text{C}$) to improve the sensitivity/selectivity of the gas sensitive coating. On the other hand, the MOSFET array

sensor contains four different sensitive areas, which have to operate at the same temperature. An optimised temperature gradient between the devices would not exceed 10°C, 5°C considered has an ideal value.

Figure 7 shows the influence of the silicon island thickness on the temperature gradient over the sensing area for a simple meander heater. A silicon island of 1.0 µm is enough to reduce the temperature gradient from 80°C to 15°C. Therefore, the two steps silicon bulk micromachining process used to fabricate the silicon island could be replaced by a high concentration boron etch stop (p⁺⁺) made by implantation.

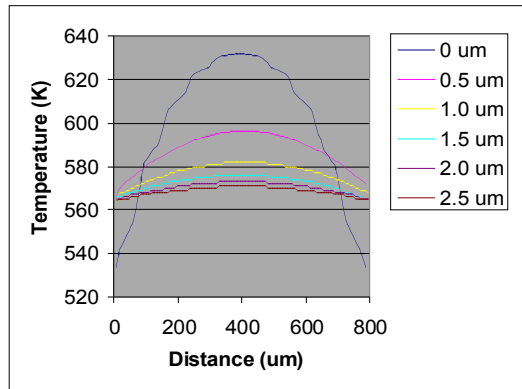


Figure 7 : Temperature distribution over the sensing area of a metal-oxide micro-hotplate as a function of the silicon island thickness.

About the MOSFET gas sensors, a silicon island with a minimum thickness of 2.0 µm provides a homogenous temperature between the different devices. The temperature gradient is lower than 5°C. An electrochemical etch-stop process could be considered to fabricate the silicon island since a boron etch-stop is not compatible with the electronic components.

5 CONCLUSION

The power consumption and the temperature distribution of micro-hotplates for gas sensing applications have been optimised by using MEMCAD to simulate their thermal behaviour. A design of micro-hotplate having a silicon island underneath the membrane was proposed to ensure a uniform temperature over the sensing area. Using FEM simulations, the thickness of the island was optimised.

The silicon island allows the design of micro-hotplates for metal-oxide gas sensors without any restrictions concerning the heater geometry. The heater and the electrodes could therefore be defined in one step using the same mask level. The silicon island makes also possible to thermally isolate electronic components. The design was used to fabricate low-power MOSFET gas sensors.

ACKNOWLEDGEMENTS

The European program Brite-Euram III (n° BRPR-CT96-0194), Nordic Sensor Technologies (NST/Sweden) and the FCAR from the Quebec Government have financially supported this project. We are grateful to IMT-samlab technical staff for the fabrication of the devices. We would like also to thank Dr. E. Scheid, LAAS, Toulouse, France, for the IR temperature measurements.

REFERENCES

- [1] A. Heilig and al., *Sensors and Actuators B*, 43, 45-51, 1997.
- [2] R.E Cavicchi and al., *Sensors and Actuators B*, 33, 142-146, 1996.
- [3] G. Faglia and al, *Sensors and Actuators B* 55, 140-146, 1999.
- [4] A. Gotz and al., *J. Micromech. Microeng*, 7, 247-249, 1997.
- [5] C. Rossi and al., *Sensors and Actuators A* 63, 183-189, 1997.
- [6] S. Astié and al., *Sensors and Actuators A* 69, 205-211, 1998.
- [7] M. Dimitrescu and al., *Proc. of Eurosensors XI*, Warsaw, Poland, Sept. 21-24, 743-746, 1997.
- [8] D. Setiadi and al., *Meeting Abstract*, Vol. 99-2, The 196th Meeting of the Electrochem. Soc., Honolulu, USA, Oct 17-22, Abstract no. 2406, 1999.
- [9] D. Briand and al., *Proc. of Eurosensors XIII*, The Hague, The Netherlands, Sept. 12-15, 703-704, 1999.
- [10] D. Briand and al., *Digest*, 10th Int. Conf. Solid-State Sensors and Actuators (Transducers'99), Sendai, Japan, June 7-10, 938-941, 1999.
- [11] D. Briand and al., to be published.
- [12] Microcosm Technologies Inc., Development Center, 101 Rogers St., Suite 213, Cambridge, MA 02142, USA.
- [13] D.J. Silversmith and al., *Proc. of the 2nd Int. Conf. on Modeling and Simulation of Microsystems (MSM'99)*, Puerto-Rico, USA, April 19-21, 613-615, 1999.
- [14] D. Briand and al., Accepted in *Sensors and Actuators B*.
- [15] I. Lundström, *Sensors and Actuators A*, 56, 75-82, 1996.
- [16] C.H. Mastrangelo and al., *Sensors and Actuators A*, 21-23, 856-860, 1990.
- [17] W-Y. Chung and al., *Digest*, 10th Int. Conf. Solid-State Sensors and Actuators (Transducers'99), Sendai, Japan, June 7-10, 672-675, 1999.
- [18] V. Guidi and al., *Sensors and Actuators B*, 49, 88-92, 1998.